The Structural and Compositional Evaluation of Some Calcium Phosphate Glasses with Bioactive Potential

DANIELA AVRAM[1], DAN UNGUREANU[2]*, NICOLAE ANGELESCU[2], IONICA IONITA[3], ANCA GHEBOIANU[4], IULIAN BANCUTA[4], ELENA CORINA POPESCU[1]

[1]Valahia University of Targoviste, Faculty of Environmental Engineering and Food Science, 2 Carol I Str., 130024 Targoviste, Romania

[2] Valahia University of Targoviste, Faculty of Materials and Mechanical Engineering, Doctoral School, Valahia University of Targoviste, 2 Carol I Str., 130024, Targoviste, Romania

[3] Valahia University of Targoviste, Faculty of Science and Arts, Department of Sciences and Advanced Technologies, 2 Carol I Str., 130024, Targoviste, Romania

[4] Valahia University of Fargoviste, Multidisciplinary Research Institute for Science and Technologies, 2 Carol I Str., 130024, Targoviste, Romania

This paper shows the experimental results of two compositional phosphocalcic glasses: 50% SiO_2 - 45% CaO - 5% P_2O_5 and 47% SiO_2 - 45% CaO - 5% P_2O_5 - 3% Ag_2O obtained through sol-gel method. In order to study their bioactivity, the two compositions were structural analyzed by X-ray diffraction method. In this case the apatite formation was highlighted after 14 days of soaked in simulated body fluid, but also other compounds ($CaCO_3$, AgCl and Ag) resulting from the same process were highlighted. The first glass composition is more bioactive than composition doped with silver. The pores of the hydrated silica network are partially clogged by the AgCl formed, which can reduce the rate of hydroxyapatite formation but this process does not cancel the bioactivity of the doped glass. The functional groups present in the structure of those two glasses before and after soaking (PO_4^{3-}, CO_3^{2-} and HO^-) were highlighted by the Fourier Transform Infrared Spectroscopy (FTIR). The elemental chemical composition was confirmed by elemental analysis WD-XRF. The particle size and the two samples stability was analyzed by Dynamic Light Scattering (DLS), Thermogravimetric Analysis (TG) and Differential Scanning Calorimetry (DSC). The granulometric analysis shows that the glass particles have average diameters of 647.9 nm for the first composition, respectively 380.4 nm for glass doped with silver. TG analysis show a total loss of weight of 8.3% for the first glass, respectively 3.72% for doped glass, which demonstrates that the two compositions are thermally stable.

Keywords: Bioactive glasses; Hydroxyapatite; WD-XRF; XRD; FTIR

The concept of bioactive material which is able to form a strong bond with the hard tissues from human body was first pointed out by Larry L. Hench, since the 1970s, with the Bioglass synthesis (45% SiO_2, 24.5% Na_2O, 24.5% CaO and 6% P_2O_5) [1].

At present one is trying to synthesize new biomaterials that can promote formation in vitro and in vivo of tissues similar of the bone, with a longer lifetime, because the average age of the population has globally increased [2, 3].

The phosphocalcic glasses are made in order to induce specific biological activity based on bioactivity and sometimes on other functional and physiological properties, such as the healing, anti-inflammatory or antimicrobial. In most of the cases, the bioactivity means creating a strong interfacial bond between implant and bone tissue, based on osteoinductive and osteoconductive property of the phosphocalcic material.

Since the discovery of Bioglass by Hench, various compositions of glasses have been studied, and also the mechanisms which lead to the bond interface formation between those two structures: implant - host tissue. However, these two aspects-bioconduction and bioinduction -led to the development of numerous clinical applications, whose development continues today [1].

At the same time, it was developed a series of bioactive glasses compositions, glass - ceramics or other bioactive ceramics based on calcium and phosphorus [4].

The use of these glasses in medical application such as orthopedics, dental or maxillofacial depends on the formation of a hydroxyapatite layer on their surface in the first days of the implantation process. The formation of this layer is a complex physico-chemical and biochemical process [4, 5].

Among various kinds of bioactive ceramics, phosphocalcic glasses obtained by sol-gel method show the high bioactivity and extraordinary ability to form strong bonds with the bone tissue, due to their high reactivity, generated by the relatively high content of SiO_2 in the composition.

In vitro testing of glasses bioactivity carried out with good results in simulated body fluid (SBF) or Kokubo solution. He synthesized for the first time this aproteic and acellular solution in 1990 [6-8].

The simulated body fluid has a similar chemical composition and *p*H of plasma and human biological fluids. Having enough Ca^{2+} and HPO_4^{2-} ions in the composition, SBF can generate and supports the de novo synthesis of hydroxyapatite on the surface of the implanted material [5, 6].

The phosphocalcic glasses doped with silver were developed in order to combat nosocomial infections, increasingly common after the bone prosthetic surgery. The antimicrobial activity of silver ions focuses a broad spectrum of microorganisms with potentially or conditionally pathogenic, without being cytotoxic to the human body in doses in which they are released by diffusion

* email: danungureanu2002@yahoo.com; Phone: 0722145165

from the porous structure of the glass. In this respect, the limitrophe area of the implant is microbiologically protected without additional risks [9-11].

Experimental part

Synthesis of sol-gel glasses

Two glasses were synthesized for this study: one from the SiO_2-CaO-P_2O_5 ternary system and another one doped with silver ions form SiO_2-CaO-P_2O_5-Ag_2O quaternary system.

The composition of bioactive glasses analyzed in this study is shown in table 1.

Table 1
COMPOSITION OF BIOACTIVE SOL-GEL GLASSES

Composition [% wt]	SiO_2	CaO	P_2O_5	Ag_2O
S_1	50	45	5	-
S_2	47	45	5	3

The phosphocalcic glasses were synthesized by sol-gel method, using the tetraethyl orthosilicate precursors ($(Si(OC_2H5)_4$ - TEOS), triethylphosphate ($(C_2H_5)_3PO_4$ - TEP), calcium nitrate tetrahydrate ($Ca(NO_3)_2 \times 4H_2O$) and silver nitrate ($AgNO_3$) - for silver-doped glass.

The glasses synthesis involves four main steps: the hydrolysis and condensation of the silicon precursors, calcium, phosphorus and silver in order to obtain the sol of glass at room temperature in a desiccator with an atmosphere saturated in moisture; gelation and maturation (aging) of the gel at 60^{0}C (fig. 1a); drying of gel (xerogel formation) at temperatures below 180^{0}C, for 48-72 h (fig. 1b) and xerogels stabilization by calcination at 600^{0}C for 8 f(fig. 1c) [11, 12].

Fig. 1. The steps of obtaining sol-gel glasses: a - aged gels, b - xerogels Ag^+, c - bioglass powder

Characterization of the samples

The structural and compositional evaluation of those two glass samples is provided by: Wavelength Dispersive X-ray Fluorescence (WD-XRF), X-ray Diffraction (XRD), Fourier Transform Infrared Spectroscopy (FTIR), Dimensional Analysis by DLS Method (dynamic light scattering), Thermal Analysis TG-DSC (thermogravimetry and differential scanning calorimetry).

The oxide chemical compositions (CaO-SiO_2-P_2O_5) were determined by Wavelength Dispersive X-ray Fluorescence Spectroscopy (WD-XRF) by using Thermo Scientific ARL Advant'X with X-ray tube (2400 W, 60kV and 80 mA), using the diffraction LiF 200 crystal [11, 12].

The structural characterization of the bioactive glass powders was performed by X-ray Diffraction (XRD) through Rigaku Ultima IV diffractometer, with the following features: scan range: 20-60^0(2θ), scan speed: 0.04 degrees/sec, the radiation source - X-ray tube (3KW power (max), U = 40KV, I = 40 mA).

The specific chemical groups from bioactive glasses were highlighted by Infrared Spectroscopy (FTIR) with Bruker Vertex 80 spectrometer with the following features: scan range: 4000-400 cm^{-1} spectral resolution 2 cm^{-1}.

The modifications occurring on the surface of the glasses was conducted before and after the soaked in simulated body fluid (SBF) for 14 days at 37^{0}C and an initial *p*H of 7.2, through XRD and FTIR analysis [13-15].

In order to increase the reactivity of the glasses, static method for bioactivity testing in vitro by soaked in SBF was chosen. Thus, the bioglass samples were maintained in SBF for 14 days without change of acellular solution, as is done in the case of the dynamic method of soaked [15-17].

The thermogravimetric (TGA) and differential scanning calorimetry (DSC) analysis for those two glasses was performed with a thermal analyzer through the coupled techniques TGA/DTA/DSC by NETZSCH STA 449 F3 JUPITER type with the temperature domain: -150^{0}C ... + 2000^{0}C, heating rate: 0.1^{0}C/min and 50^{0}C/min. The particle size of the bioactive glass was analyzed by the Zetasizer - Plus 90 - Brookhaven Instruments Corporation device, having the following characteristics: measurement domain 2 nm - 5 μm, the volume of the sample: 1-3 mL, the working temperature of 6 - 100^{0}C, angle of scattering: 15^0 - 90^{0}C.

Results and discussions

Determination of elemental composition by WD-XRF analysis

The WD-XRF analysis result for both samples of phosphocalcic glasses is shown in table 2.

Sample	Oxides [% wt]			
	SiO_2	CaO	P_2O_5	Ag_2O
S1	47.83	45.73	5.6	-
S2	48.15	41.6	5.95	3.7

Table 2
THE CHEMICAL COMPOSITION OF GLASSES

The results confirm the correctness of the synthesis method and of the technological route adopted. The moment at which the doping with silver was achieved, that is, after the addition of calcium nitrate [11], was well chosen because it was avoid the reduction of silver ions Ag^+ to metallic Ag, which significantly reduces the its antimicrobial ability [18-22].

Thermogravimetric analysis and differential scanning calorimetry

In figure 2 it is presented the thermogravimetric analysis (TG) and differential scanning calorimetry (DSC) for the sample S1.

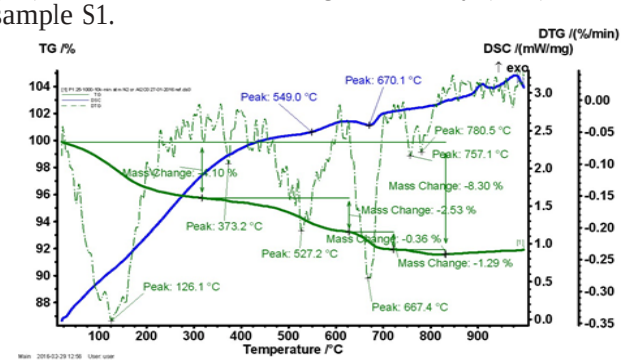

Fig. 2. Thermogravimetric analysis (TG) and Differential Scanning Calorimetry (DSC) for the sample S1

It is found that the weight loss after heating occurred in four stages: (I) 4.1% heat range 25^{0}C - 320^{0}C, (II) 2.53% in the interval 320^{0}C - 620^{0}C, (III) 0.36% to 620^{0}C - 720^{0}C and (IV) in the domain 720^{0}C 1.29% - 1000^{0}C. The total mass loss is 8.3%.

The derivative thermo-gravimetric analysis (DTG) shows an endothermic peak located at 126.1^{0}C; this corresponds

to the lost of physically adsorbed water molecules onto the surface of the glass powders and from the porous network. The endothermic peak located at 373.2^{0}C is associated with the elimination of organic wastes from glass structure. The endothermic peak located at 527.2^{0}C would correspond to the decomposition of $Ca(NO_3)_2 \cdot 4H_2O$ and decomposition (dehydroxylation) of some silanol groups, with the stabilization of the vitreous structure.

The endothermic peaks corresponding to the DTG and DSC analyzes located at 667.4^{0}C and, respectively, at 670.1^{0}C correspond to the decomposition of some precursors of calcium nitrate type in nitrogen oxides or removal of some secondary products which result from the synthesis process of bioactive glass, namely ethanol. Also, the two peaks located at 757.1 and 780.5^{0}C can be due to the same process.

In figure 3 is presented the thermogravimetric analysis (TG) and differential scanning calorimetry (DSC) for sample S2.

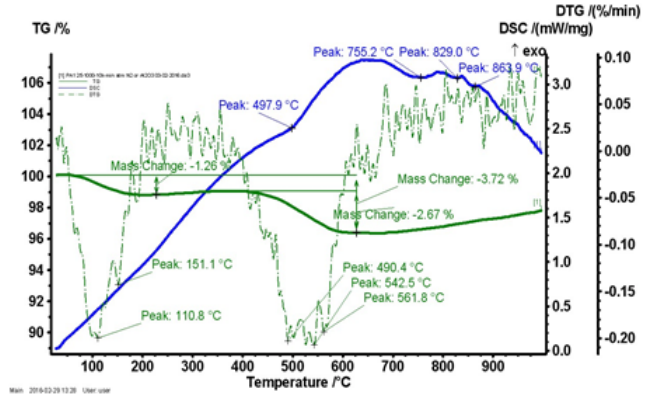

Fig. 3. Thermogravimetric analysis (TG) and differential scanning calorimetry (DSC) for sample S2

It is noted that the weight loss behind heating took place in two stages: (I): 1.26% in the range 25 - 240^{0}C and (II) 2.67% in the range 240 - 630^{0}C. The total mass loss is 3.72%.

The derived thermogravimetric analysis (DTG) reveals an endothermic peak located at 110.8^{0}C and one at 151.1^{0}C, which corresponds to the lost of physically adsorbed water molecules onto the surface of the glass powders and from the porous network.

The endotherms peaks highlighted through DTG and DSC analyzes located at 490.4^{0}C, respectively at 497.9^{0}C correspond to silver oxide decomposition with metallic silver formation. This process is carried out in a wide range of temperature (542.5 and 561.8^{0}C). Also, the two peaks located at 757.1 and at 780.5^{0}C are due to the same process.

The endothermic peaks corresponding to the DSC analysis, situated at 755.2, 829, and respectively 836.9^{0}C, correspond to the decomposition of some inorganic precursors or some byproducts, which result from the synthesis process of bioactive glass.

X-ray diffraction analysis

In figure 4 it is presented the diffractogram corresponding of samples S1 (SiO_2-CaO-P_2O_5) and S2 (SiO_2-CaO-P_2O_5-Ag_2O) before soaked in simulated body liquid at 37^{0}C and *p*H = 7.25.

At the initial moment it can be seen predominantly amorphous structure, the characteristic of vitreous materials. Only two specific peaks were assigned to hydroxyapatite at 43.77 2θ and 49.8 2θ. Other phases were identified, mostly crystalline: β-$CaCO_3$ and μ-$CaCO_3$ at peaks: 29.33 2θ and respectively 27.06 2θ and 24.96 2θ.

Along the same spectrum it has been identified mettalic Ag into S2 doped glass (38.07 2θ) as a result of

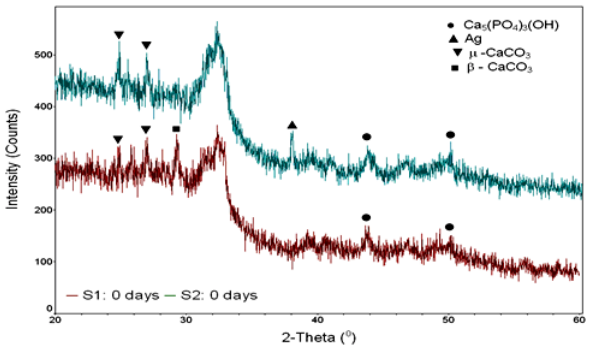

Fig. 4. X-ray diffraction spectra for S1 and S2 unsoaked glasses

decomposition of Ag_2O at 480-560^{0}C, as shown in the thermogravimetric analysis.

In figure 5 it is presented the diffractogram of samples S1 and S2 after soaked in SBF solution at 37^{0}C and *p*H 7.25 for 14 days.

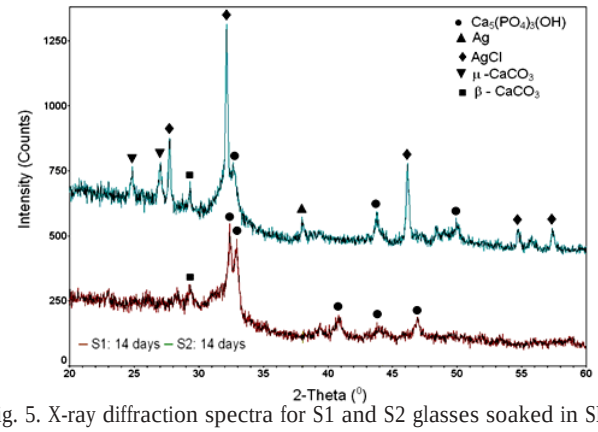

Fig. 5. X-ray diffraction spectra for S1 and S2 glasses soaked in SBF solution for 14 days

After the static soaked in acellular solution for 14 days, the formation of hydroxyapatite at surface of glass powders is observed by peaks located at 32.33 2θ; 32.9 2θ; 40.70 2θ; 43.05 2θ, 46.96 2θ, for composition S1 and 32.65 2θ; 43.05 2qθ, 49.8 2θ for composition S2.

The presence of β-$CaCO_3$ was evidenced by peaks located at 29.33 2q and for μ-$CaCO_3$ at 24.8 2θ, respectively 26.94 2θ.

The peaks located at 27.84 2θ; 32.16 2qθ; 46.2 2θ; 54.75 2θ and 57.5 2θ are associated with the formation of AgCl at the surface of silver-doped glasses. Also, metallic silver was identified in the case of soaked sample by peak from 38.07 2θ .

The presence of calcium carbonate in unsoaked glasses is due to carbonatation of the glasses samples during thermal stabilization in unprotected atmosphere (in air). In the case of the soaked samples, the increase of the intensity of those peaks is justified by the presence of $NaHCO_3$ in SBF.

The AgCl formation is due to the excess of Cl^- ions from the composition of SBF solution and the sensitivity of reaction between silver cations and chloride anions, reaction which underlies the silvermetry.

After soaked in SBF solution, glasses are found to have the ability of generating nucleation of apatite crystals on their surface, thus confirming their bioactive property [23, 24]. Also, it is found that silver remains mostly in its ionic form (Ag^+), as new formed AgCl, therefore it does not lose its antimicrobial ability [11].

FTIR analysis

In the case of two glass compositions obtained, the bioactivity study was highlighted also by Fourier Transform Infrared Spectroscopy analysis. It was taken into account the formation and development of molecular groups such

as Si-O, Si-O-Si or Si-OH common structure found in sol-gel glass structure and carbonate (CO_3^{2-}), phosphate (PO_4^{3-}) and hydroxyl (HO^-) groups present in the carbonated hydroxyapatite structure [25 - 28].

In figure 6 it is shown the FTIR spectra for samples S1 and S2 before soaking the glass powder in simulated body liquid at 37^{0}C and *p*H = 7.25.

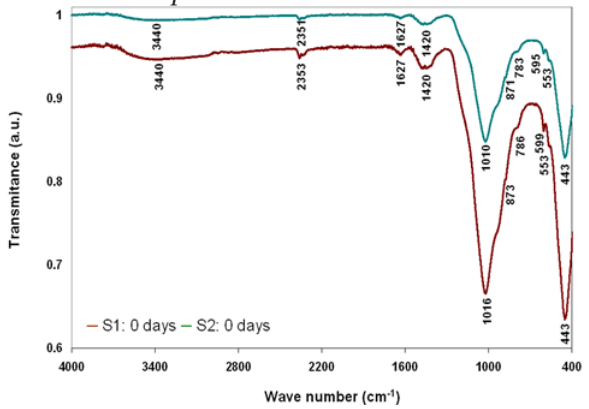

Fig. 6. FTIR spectra for S1 and S2 samples before soaking in SBF solution

The FTIR spectrum from figure 6 for the glass S1 reveals the formation of Si-O and Si-O-Si molecular group specific to the silicate network present in the glass structure obtained.

Also, the peak located at 443 cm^{-1} is characteristic to bending vibration mode of Si-O, also peak at 1016 cm^{-1} corresponding to asymmetric stretching vibration of Si-O-Si bridges.

The band located at 3440 cm^{-1} corresponds to the stretching vibrations of the HO^- molecular group and to the water associated to hydroxyapatite. The peak located at 1627 cm^{-1} corresponds to the crystallization water from the glass structure.

The presence of phosphate (PO_4^{3-}) groups was highlighted by the peaks located at 553 cm^{-1} 599 cm^{-1}, 786 cm^{-1}, respectively, 873 cm^{-1} in the glass structure. These peaks correspond to bending vibrations P-O-P, P-OH, P-O and P = O due to asymmetric bending of the PO_4^{3-} tetrahedra.

Also, the presence carbonate groups (CO_3^{2-}) in the vitrous structure was identified by the peaks located at 1420 cm^{-1} and 2353 cm^{-1}.

In the case of the S2 sample with silver, figure 6, the presence of PO_4^{3-} groups were identified at 553 cm^{-1}, 595 cm^{-1}, 783 cm^{-1}, 871 cm^{-1}. The peaks located at 1420 cm^{-1} and 2351 cm^{-1} correspond to the presence of groups carbonate (CO_3^{2-}) from the analyzed structure. The specific groups of the silicate structure Si-O and Si-O-Si are present at the peaks at 443 cm^{-1} and 1016 cm^{-1}, and those associated of the crystallisation water from the hydroxyapatite structure at the same peaks as in the case of the sample S1, respectively at 1627 cm^{-1} and 3440 cm^{-1}.

The FTIR analysis in figure 7, for the composition S1, soaked for 14 days in SBF, highlights the presence of peaks typical for the silicate network present in the glass structure.

The peak located at 443 cm^{-1} and 451 cm^{-1} is due to bending vibration mode of Si-O bridges and asymmetric stretching vibration of Si-O-Si bridges for the peak at 1001 cm^{-1}. The presence of the carbonate groups in the soaked glass structure in SBF solution, is reveald by the peaks located at 1440 cm^{-1} and 2320 cm^{-1}. Besides peaks identified in FTIR spectrum of the unsoaked sample S1, new peaks appear for specific groups: PO_4^{3-} at 484 cm^{-1}, 871 cm^{-1} and 923 cm^{-1}.

The water of crystallization associated with hydroxyapatite has been emphasized by the peak located at 1623 cm^{-1} and the vibration band HO^- from 3440 cm^{-1}. The formation of silica threedimensional network in the case of S2 glass composition, soaked for 14 days in acellular solution is highlighted in figure 7 by the peaks located at 437 cm^{-1} and 1010 cm^{-1}, specific for *symmetrical* bending vibration and asymmetrical stretching vibration modes, corresponding to Si-O-Si bridges.

The presence of phosphate groups are identified by peaks at 451cm^{-1}, 592cm^{-1}, 779cm^{-1}, 869 m^{-1} corresponding to the bending vibration modes typical for P-O-P bonds.

The peaks located at 1440 cm^{-1} and 2349 cm^{-1} show the presence of carbonate groups (CO_3^{2-}) in the structure of the S2 phosphocalcic glass - immersed in SBF (fig. 7).

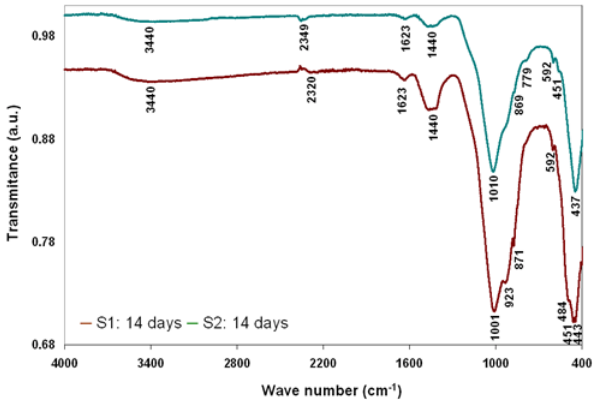

Fig. 7. FTIR spectra for S1 and S2 samples after soaking in SBF for 14 days

The peak located at 1623 cm^{-1}, and the band from 3440 cm^{-1} indicate the presence of water in the structure of S2 glass powder.

The apatite formation at the surface of glasses S1 and S2 was highlighted by the increased intensity of the phosphate peaks and appearance of new ones in the same time with the glass powders soaked over 14 days (fig. 7).

DLS analysis

Particle size analysis of S1 glass powder is presented in figure 8.

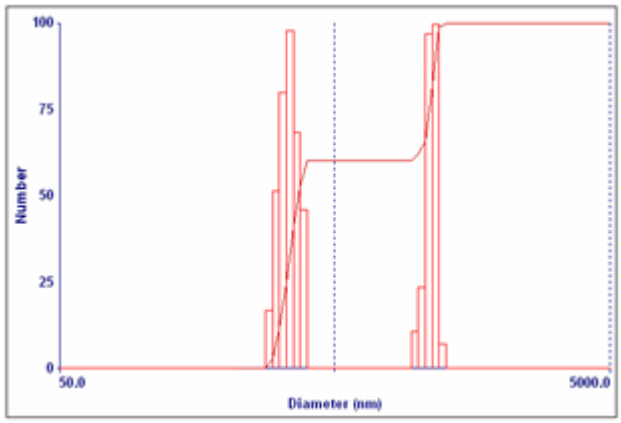

Fig. 8. Particle size analysis for S1 glass powder

The solution contains two populations of particles with diameters between 287.8 and 384.9 nm for the fist population of particles, respectively 1033.4 nm and 1230 nm, in the case of the second populations of particles. The average particle diameter is 647.9 nm. The bimodal distribution of the first composition may be due to particle agglomeration or to an insufficient processing in the previous steps.

In the case of S2 glass powder, DLS analysis shows, in figure 9, a unimodal distribution. The same analysis

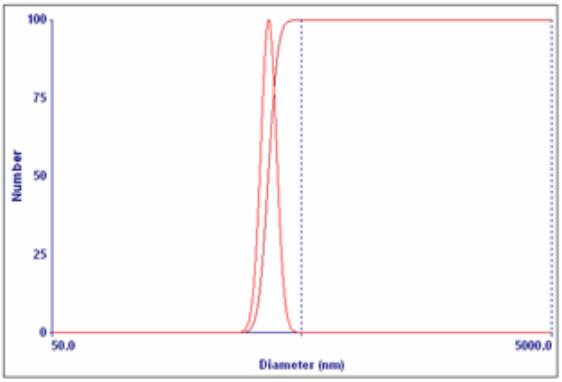

Fig. 9. Particle size analysis for the S2 glass powder

revealed particles with diameters between 338.7 and 427.3 nm with a maximum at 380.4 nm. The average particle diameter is 380.4 nm.

Conclusions

Two glass compositions from the SiO_2-CaO-P_2O_5 and SiO_2-CaO-P_2O_5-Ag_2O by sol-gel method with relatively low production costs were obtained.

The X-ray fluorescence spectroscopy confirmed a chemical composition. The results obtained are very close to the theoretical ones calculated for both synthesized samples, which confirms the correctness of the technological synthesis route adopted.

Doping with silver did not prevent coalescence of the particles, so the formation of sol, and neither the reduction of the ionic silver to metallic silver, which would reduce the antimicrobial ability of the doped glass.

From the thermogravimetric analysis of those two glass powder, it is found a total loss of weight of 8.3% for glass S1, respectively 3.72% for glass S2, which demonstrates that the two compositions are thermally stable.

The composition S2 doped with silver is more stable than S1, a fact demonstrated by the mass loss lower in only two steps, for the sample S1. This can be attributed to the silver introduced in the silico-phosphate tetrahedral network and to the formation of metallic silver at 490.4^0C - 561.8^0C.

The bioactivity of the glasses was revealed by XRD analysis. The data analysis shows different reactivity degrees of the two compositions. The hydroxyapatite formation was highlighted for both compositions after immersion in SBF solution.

The formation of $CaCO_3$ after the samples were soaked can be attributed to saturation of the SBF in Ca^{2+} and HCO_3^- ions and decrease of *p*H value. This phenomenon promotes the precipitation of compounds with basic *p*H.

In the case of S2 glass composition it can be observed the AgCl formation in considerable quantities, which is explained by diffusion of Ag ions in the vitreous matrix much more easily and their reaction with chloride anions, Cl^-, present in extremely large amounts in simulant body fluid composition (221.7 mmol/L).

The pores of the hydrated silica network are partially clogged by the AgCl formed, which can reduce the rate of hydroxyapatite formation but this process does not cancel the bioactivity of the doped glass. The glass S1 is more bioactive than composition S2. According to the diffractogram from figure 5, it is possible that some of the hydroxyapatite peaks be masked by the newly formed AgCl, as in the case of the peak at 32.16 2θ and at 46.2 2θ.

The FTIR analysis of the two glasses confirms the presence of PO_4^{3-}, CO_3^{2-} groups and HO^- specific for hydroxyapatite and carbonated hydroxyapatite in the composition of soaked samples in SBF, and the presence of Si-O and Si-O-Si groups which are characteristic to the SiO_2-CaO-P_2O_5 glasses. The water of crystallisation is confirmed by the presence of peak at 1627 cm^{-1}, confirming the formation of the carbonated hydroxyapatite which is specific of bone tissue.

The XRD and FTIR analyzes show that the formation of the implant-tissue interfacial bond is initiated in vitro at 14 days after soaking in SBF, and by extrapolation it can be followed in vivo after about 14 days from surgery.

The granulometric analysis shows that the glass particles have average diameters of 647.9 nm - for the composition S1, respectively 380.4 nm for S2. This shows that glass powders have large specific surface area; this aspect has positive implications in terms of bioactive potential of the glasses.

References

1.HENCH, L.L., WILSON, J., An Introduction to Bioceramics, World Scientific, Singapore, 1993.
2.PEREZ, GONZALEZ, J.A., Síntesis de biovidrios por la técnica sol-gel con incorporación de metales y estudio de sus propiedades antibacteriales, Ph.D. Thesis, Universidad de Chile, Departamento de Ingeniería Química y Biotecnología, 2012.
3.HENCH, L.L., Biomaterials, 19, 1998, p. 1419.
4.JUN, IK, SONG, J.H., CHOI, W.Y., KOH, Y.H., KIM, H.E., KIM, H.W., J. Am. Ceram. Soc. 90, 2007, p. 2703.
5.MAMI, M., LUCAS-GIROT A, OUDADESSE, H., DIETRICH, E., J. Applied Surface Science, 254, 2008, p. 7386.
6.KOKUBO, T., KUSHITANI, H., SAKKA, S., KITSUGI, T., YAMAMURO, T., J. Biomed. Mater. Res., 24, 1990, p. 721.
7.OHTSUKI, C., KUSHITANI, H., KOKUBO, T., KOTANI, S., YAMAMURO, T., J. Biomed. Mater. Res., 25, 2001, p. 1363.
8.ABE, Y., KAWASHITA, M., KOKUBO, T., NAKAMURA, T., J. Ceram. Soc. Japan, 109, 2001, p. 106.
9.BELLATONE, M., WILLIAMS, H.D., HENCH, L.L., Antim. Ag. Ch., 46, 2002, p. 1940.
10.JONES, J.R., LEE, P.D., HENCH, L.L., Phil.Trans. R. Soc. A., 364, 2006, p. 263.
11.AVRAM, D., ANGELESCU, N., UNGUREANU, D.N., BRATU, V., Journal of Optoelectronics and Adv. Mat., 17, 2015, p.1038.
12.AVRAM, D., ANGELESCU, N., UNGUREANU, D.N., GHEBOIANU, A., BANCUTA, I., SETNESCU, T., Journal of Optoelectronics and Adv. Mat., 18, 2016, p. 691.
13.HENCH, L.L., ANN, N.Y., Acad. Sci., 523, 1998, p. 54.
14.ZHONG, J., GREENSPAN, D.C., J. Biomed. Mater. Res., 53, 2000, p. 694 – 601.
15.HENCH, L.L., Bioactive Ceramics, in Bioceramics: Material Characteristics vs In Vivo Behaviour. P. Ducheyne and J. Lemons (Eds) Annals of N.Y. Academy of Science, New York, 523, 1998, p. 54.
16.FALAIZE, S., RADIN, S., DUCHEYNE, P., J. Am. Ceram. Soc., 82, 1999, p. 969.
17.RAMILA, A., VALLET-REGÍ, M., Biomaterials, 22, 2001, p. 2301.
18.GEYER, G., SCHOTT, C., SWARZKOPF, A., HNO 47, 1999, p. 25.
19.GHANDOUR, W., HUBBARD, J.A., DEISTRUNG, J., HUGHES, M.N., POOLE, R.K., Appl. Microbiol. Biotechnol, 28, 1988, p. 314.
20.GRIER, N., (1991) Disinfection, sterilization and preservation. Lea & Febiger, Philadelphia, PA, p. 68.
21.GRISTINA, A.G., Science, 237, 1987, p. 1588.
22.GUPTA, A., SILVER, S., Nat. Biotechnol., 16, 1998, p. 888.
23.OHTSUKI, C., KOKUBO, T., YAMAMURO, T., Mechanism of Apatite Formation on CaO - SiO_2 - P_2O_5 Glasses in a Simulated Body Fluid-J. Non-Cryst. Solids 143, 1992, p. 84-92.
24.KOKUBO, T., CHO, S.B., NAKANISHI, K., OHTSUKI, C., KITSUGI, T., YAMAMURO, T., NAKAMURA, T., Dependence of bone-like apatite formation on structure of silica gel, Bioceramics, 7, 1994, p. 49-54.
25.AVRAM, D., UNGUREANU, D.N., ANGELESCU, N., GHEBOIANU, A., BANCUTA, I., BRATU, M.G., The Scientific Bulletin of Valahia University - Materials and Mechanics, 10, 2015, p. 81-86.
26.CUNEYT, TAS A., Ceram. Eng. Sci. Proc., 30, 2009, p. 139.
27.SABOORI, A., RABIEE, M., MOZTARZADEH, F., SHEIKHI, M., TAHRIRI, M., KARIMI, M., Mater. Sci. Eng., C 29, 2009, p. 335.
28.ALMEIDA, R.M., GAMA, A., VUEVA, Y., J. Sol-Gel Sci. Technol., 57, 2009, p. 336.

Manuscript received: 25.09.2017